OPTIMAL FEEDBACK RENDEZVOUS IN ELLIPTIC ORBITS ACCOUNTING FOR NONLINEAR DIFFERENTIAL GRAVITY

Rajnish Sharma[*], Prasenjit Sengupta[†] and Srinivas R. Vadali[‡]

Department of Aerospace Engineering
Texas A&M University
3141 TAMU
College Station, TX 77843-3141

ABSTRACT

This paper presents a novel approach to the design of optimal feedback control laws, for minimum-fuel rendezvous between satellites in elliptic orbits of arbitrary eccentricity. The rendezvous problem for the nonlinear differential gravity model is solved by the application of neighboring optimal feedback control methodology used in conjunction with a nominal trajectory, obtained by solving the related minimum-fuel feedback control problem for the linear Tschauner-Hempel equations, analytically. This novel closed-form solution is used to determine the best values of the final true anomaly by examining its effect on the cost-to-go for rendezvous. The optimal control law accounting for nonlinear differential gravity is obtained by using a generalized sweep method, valid when the reference solution does not satisfy the first-order necessary conditions for optimality, exactly. Several numerical examples are analyzed to demonstrate the efficacy of the method.

Key Words: - Tschauner-Hempel equations, Perturbation control, Rendezvous, Sweep method.

INTRODUCTION

The problem of satellite rendezvous in orbits around a planet continues to provoke great interest due to its utility in spacecraft servicing, assembly, and inspection. The most basic model for the study of relative motion is given by the Hill-Clohessy-Wiltshire

[*] Ph.D. Candidate, Student Member AIAA, Email: aeroraj@neo.tamu.edu
[†] Ph.D. Candidate, Student Member AIAA, Email: prasenjit@neo.tamu.edu
[‡] Stewart & Stevenson-1 Professor, Associate Fellow AIAA, Email: svadali@aero.tamu.edu

(HCW) equations [1, 2]. These equations model relative motion between a chaser and target vehicle under the assumptions of circular target orbit, linear differential gravity field, and two-body dynamics. The HCW equations constitute a sixth-order, linear model, which is extremely useful for preliminary analysis. However, the scope of this model is severely limited and it is unreliable when the target orbit is eccentric and the distance between the chaser and target is not negligible when compared to that of the target from the gravitational center. In order to study the optimal rendezvous problem rigorously, it is necessary to model eccentricity and nonlinearity effects. A vast body of literature exists on the study of relative motion dynamics for the two-body problem when the HCW assumptions are violated.

Knollman and Pyron [3] and London [4] obtained approximate solutions to the HCW equations, perturbed by second-order nonlinearities. Karlgaard and Lutze [5] also obtained analytical relative motion equations near a circular orbit that are correct to second-order, using spherical coordinates. Richardson and Mitchell [6] used perturbation analysis to obtain the solution valid for third-order nonlinearities by enforcing periodicity conditions on the linear solution.

The effect of eccentricity on the relative motion equations has been studied both for the linear as well as nonlinear equations. The linear problem for eccentric reference orbits was introduced by Tschauner and Hempel [7]. The Tschauner-Hempel (TH) equations use true anomaly of the target as the independent variable, rather than time, and the local position of the chaser is normalized by the radial distance of the target. Analytical expressions for relative motion were obtained by de Vries [8], who treated eccentricity as a perturbation to the TH equations. In his approach, only terms of up to

first-order in eccentricity were considered. The TH equations by themselves admit analytical solutions in the form of special integrals as shown in Refs. 9–11. These solutions are valid for arbitrary eccentricities and have been used for the determination of state transition matrices for linearized relative motion with true anomaly as the independent variable [12–15]. Melton [16] and Broucke [17] have developed state transition matrices for relative motion with time as the independent variable. Reference 16 uses a series expansion for radial distance and true anomaly, in terms of time. However, for moderate eccentricities, the convergence of such series requires the inclusion of higher-order terms. Attempts were made by Euler and Shulman [18] to obtain solutions to the TH equations with second-order gravitational perturbations in order to enhance their domain of applicability to large relative distances and arbitrary eccentricity. Although the authors noted the nonexistence of an analytical solution to this problem at that time, in a recent work [19], such a solution has been presented for the special case of periodic motion.

The optimal rendezvous problem is also of historical interest, especially due to Lawden's primer vector theory [9]. Billik [20] used a differential games approach to design optimal thruster programming laws for the HCW equations. Euler [21] approached the rendezvous problem by attempting to find an open-loop optimal control to the TH equations, for the standard quadratic cost function valid for power-limited, low-thrust propulsion. However, a complete analytical solution could not be found, and results were obtained by restricting the equations to first-order in eccentricity. Edelbaum [22] formulated and solved the optimal rendezvous problem in terms of small orbital element differences. Gobetz [23] also used a similar linearization in orbital element space, with

the additional assumption of a near-circular target orbit, but used a nonsingular element set that extended the validity of the laws to those cases where eccentricity and inclination are zero – known singularities in the classical orbital element set. The elements used by Gobetz are similar to the equinoctial elements [24]. Jezewski and Stoolz [25] formulated the constant-thrust orbital transfer problem, by expressing the gravity field as a third-order polynomial in time by using two measurements of position and velocity and solving for the polynomial coefficients. Solutions to the continuous-thrust optimal rendezvous problem in a linearized gravity field using the TH equations, have been explored extensively in Refs. 10, 26, and 27. In recent work by Zanon and Campbell [28], an approximate solution for an open-loop, bounded-input controller was developed using spline function approximations for certain key integrals. Palmer [29] presented an analytical formulation for optimal transfer paths based on the HCW equations.

Various methods for the treatment of nonlinearity in the optimal rendezvous problem have been proposed. Williams [30] presented a quasilinearization scheme for spacecraft rendezvous on small relative inclination orbits by using tethers. Park et al. [31] proposed a feedback controller for the nonlinear optimal rendezvous of a spacecraft near a circular orbit by using Hamilton-Jacobi theory. Kim and Spencer [32] demonstrated the use of genetic algorithms to solve for Hohmann and bi-elliptical transfers.

The study of the literature on the optimal rendezvous problem reveals that analytical solutions for arbitrary eccentricity as well as nonlinear differential gravity have not been obtained. The necessity for such solutions arises from recent interest in formations in highly elliptic orbits, such as the Magnetosphere Multiscale Mission [33,34]. Moreover, the solutions to the optimal rendezvous problem obtained by accounting for the above

mentioned perturbations will typically require lower costs since the physics of the problem is accurately reflected in the model.

This paper begins by presenting the nonlinear TH equations in nondimensional form where a perturbation parameter, which captures the effect of nonlinearity as well as eccentricity of the reference orbit, is identified. Next, a novel analytical solution is presented for the minimum-fuel rendezvous problem for the non-autonomous linear model obtained by setting the perturbation parameter to zero. Finally, the optimal control problem is posed for nonzero values of the perturbation parameter. Its solution, accurate to first-order, is obtained in feedback form [35-37] to meet the terminal constraint for rendezvous, accurately. The results are validated on the fully nonlinear model. Several examples for various combinations of eccentricity and initial separation distance are presented to demonstrate the excellent performance and wide applicability of the proposed methodology.

EQUATIONS OF MOTION

The nonlinear (dimensional) rendezvous equations are:

$$\ddot{\xi} - 2\dot{\theta}\dot{\eta} - \dot{\theta}^2\xi - \ddot{\theta}\eta = -\frac{\mu(r+\xi)}{\left[(r+\xi)^2 + \eta^2 + \zeta^2\right]^{3/2}} + \frac{\mu}{r^2} + U_\xi \tag{1}$$

$$\ddot{\eta} + 2\dot{\theta}\dot{\xi} - \dot{\theta}^2 y + \ddot{\theta}\xi = -\frac{\mu\eta}{\left[(r+\xi)^2 + \eta^2 + \zeta^2\right]^{3/2}} + U_\eta \tag{2}$$

$$\ddot{\zeta} = -\frac{\mu\zeta}{\left[(r+\xi)^2 + \eta^2 + \zeta^2\right]^{3/2}} + U_\zeta \tag{3}$$

where, ξ, η, and ζ indicate respectively, the radial, along-track, and out-of-plane components of the position vector of the chaser satellite in the target satellite's Local-Vertical-Local-Horizontal (LVLH) frame; and U_ξ, U_η, and U_ζ indicate the components of the control acceleration vector along the respective directions. In the above equations, time is the independent variable. Furthermore, $(\dot{})$ and $(\ddot{})$, respectively, denote the first and second derivative with respect to time. To convert the rendezvous equations into the TH form, the following steps are performed:

1. The independent variable is changed from time to true anomaly, denoted by f. Therefore,

$$(\dot{}) = \dot{f}(') = \bar{n}(1+e\cos f)^2(') \tag{4}$$

$$(\ddot{}) = \dot{f}^2('') + \ddot{f}(') = \bar{n}^2(1+e\cos f)^3[(1+e\cos f)('') - 2e\sin f(')] \tag{5}$$

where $\bar{n} = \sqrt{\mu/p^3}$, $p = a(1-e^2)$ is the semi-parameter of the target orbit and $(')$ and $('')$ denote the first and second derivative with respect to f, respectively.

2. Next, nondimensional position variables are defined as follows: $x = (1+e\cos f)\xi/\rho_0$, $y = (1+e\cos f)\eta/\rho_0$, and $z = (1+e\cos f)\zeta/\rho_0$, where, ρ_0, the size of the relative orbit, is used as a characteristic length. The nondimensional control acceleration components are given by the following: $u_x = U_\xi/(\rho_0\bar{n}^2)$, $u_y = U_\eta/(\rho_0\bar{n}^2)$ and $u_z = U_\zeta/(\rho_0\bar{n}^2)$.

3. Finally, let $\varepsilon = \rho_0/p$ be the nonlinearity measure of the system. The degree of nonlinearity not only depends on the size of the relative orbit, but also on the eccentricity of the reference orbit, introduced through the semi-parameter.

After performing the above steps, the state-space representation of the TH equations can be obtained with $\mathbf{x} \in \mathbb{R}^{6\times 1} \equiv [x; y; z; x'; y'; z']^T$, as follows:

$$\mathbf{x}' = \mathbf{h}(\mathbf{x}, f) + B(f)\mathbf{u}\,, \tag{6}$$

where $\mathbf{u} \in \mathbb{R}^{3\times 1} \equiv [u_x; u_y; u_z]^T$. In more explicit form, the components of the above vector equation can be written as shown below:

$$x' = v_1 \tag{7}$$

$$y' = v_2 \tag{8}$$

$$z' = v_3 \tag{9}$$

$$v_1' = 2v_2 + \frac{x}{(1+e\cos f)} + \frac{1}{(1+e\cos f)}\frac{1}{\varepsilon}\left\{1 - \frac{(1+\varepsilon x)}{\left[(1+\varepsilon x)^2 + \varepsilon^2 y^2 + \varepsilon^2 z^2\right]^{3/2}}\right\} + \frac{u_x}{(1+e\cos f)^3} \tag{10}$$

$$v_2' = -2v_1 + \frac{y}{(1+e\cos f)} - \frac{1}{(1+e\cos f)}\frac{y}{\left[(1+\varepsilon x)^2 + \varepsilon^2 y^2 + \varepsilon^2 z^2\right]^{3/2}} + \frac{u_y}{(1+e\cos f)^3}$$

(11)

$$v_3' = -\frac{e\cos f}{(1+e\cos f)}z - \frac{1}{(1+e\cos f)}\frac{z}{\left[(1+\varepsilon x)^2 + \varepsilon^2 y^2 + \varepsilon^2 z^2\right]^{3/2}} + \frac{u_z}{(1+e\cos f)^3} \tag{12}$$

THE NOMINAL SOLUTION

A key component of the work that is reported in this paper is the determination of the analytical reference solution to a special case of the main problem. This reference solution and a special choice of a perturbation parameter lead to an accurate solution to the main optimal control problem. A good reference solution is essential for fast convergence of Taylor series expansions about it. Before proceeding further it is noted

that the integral sum of squares of the control accelerations is utilized as the performance index. This form of the performance index is appropriate for power-limited, low-thrust propulsion [38]. The next section provides the closed-form solution for the nominal linear-quadratic (LQ) optimal control problem.

Analytical Solution for the LQ Problem

The linear part of the TH equations can be obtained by taking the limit of Eq. (6) as $\varepsilon \to 0$. The linear TH equations in state-space representation are given below:

$$\mathbf{x}' = A(f)\mathbf{x} + B(f)\mathbf{u} \tag{13}$$

where, $\mathbf{x} \in \mathbb{R}^6, u \in \mathbb{R}^3, A : \mathbb{R}_{\geq 0} \to \mathbb{R}^{6\times 6}, B : \mathbb{R}_{\geq 0} \to \mathbb{R}^{6\times 3}$, and

$$\mathbf{x} = [x; y; z; x'; y'; z']^T, \quad B(f) = (1 + e\cos f)^{-3} \begin{bmatrix} 0_{3\times 3} \\ 1_{3\times 3} \end{bmatrix}$$

$$A(f) = \begin{bmatrix} 0 & 0 & 0 & 1 & 0 & 0 \\ 0 & 0 & 0 & 0 & 1 & 0 \\ 0 & 0 & 0 & 0 & 0 & 1 \\ \dfrac{3}{(1+e\cos f)} & 0 & 0 & 0 & 2 & 0 \\ 0 & 0 & 0 & -2 & 0 & 0 \\ 0 & 0 & -1 & 0 & 0 & 0 \end{bmatrix} \tag{14}$$

Note that the actual control acceleration $\mathbf{U}$ is obtained from

$$\mathbf{U}(f) = \rho_0 \overline{n}^2 \mathbf{u}(f) \tag{15}$$

The LQ optimal control problem is posed as the follows:

Minimize:

$$J = \frac{1}{2} \int_{f_0}^{f_T} (\mathbf{u}^T R \mathbf{u}) df \tag{16}$$

subject to Eq. (13) and initial and final conditions as given below:

$$\mathbf{x}(f_0) = \mathbf{x}_0; \mathbf{x}(f_T) = \mathbf{x}_T \tag{17}$$

Note that the weight matrix R in Eq. (16) is positive definite. For the LQ problem posed, it can be shown that the necessary conditions for optimality [39] yield the following relations for the controls and costates, denoted by $\boldsymbol{\lambda}$:

$$\begin{aligned} \boldsymbol{\lambda}' &= -A^T\boldsymbol{\lambda}; \\ \mathbf{u} &= -R^{-1}B^T\boldsymbol{\lambda} \end{aligned} \tag{18}$$

The solution to the augmented linear system comprised of states and costates can be obtained using the state transition matrix (STM), Φ, as shown below:

$$\begin{bmatrix} \mathbf{x}' \\ \boldsymbol{\lambda}' \end{bmatrix} = \begin{bmatrix} A & -BR^{-1}B^T \\ 0_{6\times 6} & -A^T \end{bmatrix} \begin{bmatrix} \mathbf{x} \\ \boldsymbol{\lambda} \end{bmatrix} \Rightarrow \begin{bmatrix} \mathbf{x}(f) \\ \boldsymbol{\lambda}(f) \end{bmatrix} = \Phi(f, f_0) \begin{bmatrix} \mathbf{x}(f_0) \\ \boldsymbol{\lambda}(f_0) \end{bmatrix} \tag{19}$$

Consequently, the initial values of $\boldsymbol{\lambda}$ can be determined as follows:

$$\Phi = \begin{bmatrix} \Phi_{xx} & \Phi_{x\lambda} \\ \Phi_{\lambda x} & \Phi_{\lambda\lambda} \end{bmatrix} \Rightarrow \boldsymbol{\lambda}(f_0) \equiv \boldsymbol{\lambda}_\mathbf{0} = \Phi_{x\lambda}^{-1}(f_T, f_0)[\mathbf{x}_T - \Phi_{xx}(f_T, f_0)\mathbf{x}_0] \tag{20}$$

Thus, the LQ problem can be solved if Φ_{xx}, $\Phi_{\lambda\lambda}$ and $\Phi_{x\lambda}$ are determined.

While not immediately obvious, the required sub-matrices can be evaluated analytically by using the closed-form solutions of the TH equations. The solutions to the unforced TH equations are given in Ref. 14:

$$x(f) = c_1 \cos f(1+e\cos f) + c_2 \sin f(1+e\cos f) + \frac{2c_3}{\eta^2}\left[1 - \frac{3e}{2\eta^3}\sin f(1+e\cos f)K(f)\right] \tag{21}$$

$$y(f) = -c_1 \sin f(2+e\cos f) + c_2 \cos f(2+e\cos f) - \frac{3c_3}{\eta^5}(1+e\cos f)^2 K(f) + c_4 \tag{22}$$

$$z(f) = c_5 \cos f + c_6 \sin f \tag{23}$$

where c_1, c_2, c_3, c_4, c_5 and c_6 are constants of integration , and

$$K(f) \equiv \int_{f_0}^{f} \frac{\eta^3}{(1+e\cos f)^2} df = \left(E - e\sin E\right) - \left(E_0 - e\sin E_0\right) = n\,\Delta t \tag{24}$$

The function $K(f)$, denoting scaled time since epoch, is easier to evaluate in terms of eccentric anomaly, *E*. The following equations show the relationships between eccentric and true anomalies [40]:

$$\begin{aligned} \cos f &= \frac{\cos E - e}{1 - e\cos E}, \sin f = \frac{\eta \sin E}{1 - e\cos E} \\ \cos E &= \frac{\cos f + e}{1 + e\cos f}, \sin E = \frac{\eta \sin f}{1 + e\cos f} \end{aligned} \tag{25}$$

The following expressions are also provided in Ref. 14:

$$\begin{aligned} x'(f) &= -c_1(\sin f + e\sin 2f) + c_2(\cos f + e\cos 2f) \\ &- \frac{3ec_3}{\eta^2}\left[\frac{\sin f}{1+e\cos f} + \frac{1}{\eta^3}(\cos f + e\cos 2f)K(f)\right] \end{aligned} \tag{26}$$

$$y'(f) = -c_1(2\cos f + e\cos 2f) - c_2(2\sin f + e\sin 2f) - \frac{3c_3}{\eta^5}\left[\eta^3 - e(2\sin f + e\sin 2f)K(f)\right] \tag{27}$$

$$z'(f) = -c_5 \sin f + c_6 \cos f \tag{28}$$

Calculations are simplified if the in-plane problem, pertaining to motion in the x and y directions, and out-of-plane problem, pertaining to motion in the z direction, are treated separately. As shown in Ref. 19, the relationship between the states and the integration constants can be expressed as $\mathbf{x} = L(f)\mathbf{c}$; where, the entries of the matrix L can be obtained from the terms corresponding to the constants of integration in Eqs. (21-23) and Eqs. (26-28), with the notation: $\mathbf{c} = [c_1, c_2, c_3, c_4, c_5, c_6]^T$. This matrix has determinant equal to 1, and the constants of integration can then be calculated by its adjoint, in terms of the initial condition vector $\mathbf{x}_0$, as shown below:

$$c_1 = -\frac{3}{\eta^2}(e+\cos f_0)x_0 - \frac{1}{\eta^2}\sin f_0(1+e\cos f_0)x_0' - \frac{1}{\eta^2}(e+2\cos f_0 + e\cos^2 f_0)y_0' \tag{29}$$

$$c_2 = -\frac{3}{\eta^3}\frac{\sin f_0(1+e\cos f_0+e^2)}{(1+e\cos f_0)}x_0 + \frac{1}{\eta^2}(\cos f_0 - 2e + e\cos f_0)x_0' - \frac{1}{\eta^2}\sin f_0(2+e\cos f_0)y_0' \tag{30}$$

$$c_3 = l_1 x_0 + l_2 x_0' + l_3 y_0' \tag{31}$$

$$c_4 = -\frac{1}{\eta^2}(2+e\cos f_0)\left[\frac{3e\sin f_0}{(1+e\cos f_0)}x_0 + (1-e\cos f_0)x_0' + e\sin f_0 y_0'\right] + y_0 \tag{32}$$

$$c_5 = (\cos f_0)z_0 - (\sin f_0)z_0' \tag{33}$$

$$c_6 = (\sin f_0)z_0 + (\cos f_0)z_0' \tag{34}$$

where,

$$\begin{aligned} l_1 &= 2 + 3e\cos f_0 + e^2 \\ l_2 &= e\sin f_0(1+e\cos f_0) \\ l_3 &= (1+e\cos f_0)^2 \end{aligned} \tag{35}$$

Equations (29-34) may be rewritten as $\mathbf{c} = M(f_0)\mathbf{x}_0$ where $M = adj(L)$. Using the above equations, the solution for Φ_{xx} can be written as:

$$\begin{aligned} &\mathbf{x}(f) = L(f)M(f_0)\mathbf{x}_0 \\ &\Rightarrow \Phi_{xx}(f, f_0) = L(f)M(f_0) \end{aligned} \tag{36}$$

The remaining blocks of the STM can be obtained by observing that the Hamiltonian system, Eq. (19), leads to a state transition matrix that is symplectic in nature. More specifically, if $\Im$ denotes the symplectic matrix of appropriate order, Eqs. (19-20) imply

$$\begin{aligned} &\Phi\Im\Phi^T = \Im \\ &\text{or, } \begin{bmatrix} \Phi_{xx} & \Phi_{x\lambda} \\ \Phi_{\lambda x} & \Phi_{\lambda\lambda} \end{bmatrix}\begin{bmatrix} 0_{6\times6} & I_{6\times6} \\ -I_{6\times6} & 0_{6\times6} \end{bmatrix}\begin{bmatrix} \Phi_{xx}^T & \Phi_{\lambda x}^T \\ \Phi_{x\lambda}^T & \Phi_{\lambda\lambda}^T \end{bmatrix} = \begin{bmatrix} 0_{6\times6} & I_{6\times6} \\ -I_{6\times6} & 0_{6\times6} \end{bmatrix} \end{aligned} \tag{37}$$

Resolving the matrix multiplication and comparing the block matrices on both sides leads to four equations, one of which is given below:

$$\Phi_{xx}\Phi_{\lambda\lambda}^{T} - \Phi_{x\lambda}\Phi_{\lambda x}^{T} = I_{6\times 6} \tag{38}$$

If $\mathbf{x}$ is not present in the cost function, Eq. (16) (as is the case considered here), then $\boldsymbol{\lambda}'$ does not depend on $\mathbf{x}$ explicitly. In such a case, $\Phi_{\lambda x} = 0_{6\times 6}$ and it follows that:

$$\Phi_{\lambda\lambda}(f, f_0) = \Phi_{xx}^{T}(f_0, f) = M^{T}(f)L^{T}(f_0) \tag{39}$$

From Eq. (19) and Eq. (6b), the solution to the forced system is:

$$\begin{aligned}\mathbf{x}(f) &= \Phi_{xx}(f, f_0)\mathbf{x}_0 - \int_{f_0}^{f} \Phi_{xx}(f, s)B(s)R^{-1}B^{T}(s)\Phi_{\lambda\lambda}(s, f_0)\boldsymbol{\lambda}_0 ds \\ &= \Phi_{xx}(f, f_0)\mathbf{x}_0 + \Phi_{x\lambda}(f, f_0)\boldsymbol{\lambda}_0\end{aligned} \tag{40}$$

Hence,

$$\Phi_{x\lambda}(f, f_0) = -\int_{f_0}^{f} \Phi_{xx}(f, s)B(s)R^{-1}B^{T}(s)\Phi_{\lambda\lambda}(s, f_0)\boldsymbol{\lambda}_0 ds \tag{41}$$

It can be shown by substituting Eq. (39) into Eq. (41) that:

$$\begin{aligned}\Phi_{x\lambda}(f, f_0) &= -L(f)\left(\int_{f_0}^{f} M(s)B(s)R^{-1}B^{T}(s)M^{T}(s)ds\right)L^{T}(f_0) \\ &= -L(f)[N(f) - N(f_0)]L^{T}(f_0)\end{aligned} \tag{42}$$

where,

$$N(f) = \int M(f)B(f)R^{-1}B^{T}(f)M^{T}(f)df \tag{43}$$

It is evident that the problem can be solved completely if $N(f)$ is evaluated. It is also worth noting that $N(f)$ is symmetric and it can be shown that

$$B(f)R^{-1}B^T(f) = (1+e\cos f)^{-6}\begin{bmatrix} 0 & 0 \\ 0 & R^{-1} \end{bmatrix} \tag{44}$$

Though it appears at the outset that the integration process is complicated due to the presence of terms containing $(1+e\cos f)$ in the denominator, integration can be performed by changing the independent variable to E. Consequently, $N(f)$ may be rewritten as:

$$N(f) = N^{(3)}(f)K^3(f) + N^{(2)}(f)K^2(f) + N^{(1)}(f)K(f) + N^{(0)}(f) \tag{45}$$

The components of $N^{(0..3)}(f)$ are presented as Appendix I. For the sake of brevity the following definition is used:

$$\bar{N}(f_T, f_0) \triangleq N(f_T) - N(f_0) \tag{46}$$

Dependence of the Cost-to-go on the Final Value of True Anomaly

For given initial and final conditions, $\mathbf{x}_0$ and $\mathbf{x}_T$, and epoch f_0, the cost is a function of the final value of true anomaly, f_T. Using Eqs. (16) and (18), we obtain the following representation of the cost function:

$$\begin{aligned} J^*(f_T) &= \frac{1}{2}\int_{f_0}^{f_T} \boldsymbol{\lambda}^T B(f)R^{-1}B(f)^T \boldsymbol{\lambda} df \\ \Rightarrow &\frac{1}{2}\int_{f_0}^{f_T} \boldsymbol{\lambda}_0^{\mathrm{T}} \Phi_{\lambda\lambda}^T(f, f_0)B(f)R^{-1}B(f)^T \Phi_{\lambda\lambda}^T(f, f_0)\boldsymbol{\lambda}_0 df \end{aligned} \tag{47}$$

The following definitions are used for ease of notation: $L(f_0) = L_0, L(f_T) = L_T, M(f_0) = M_0$ and $M(f_T) = M_T$. Furthermore, since $\boldsymbol{\lambda}_0$ is a constant, the use of Eqs. (39), (43), and (46) results in the following:

$$J^* = \frac{1}{2}\boldsymbol{\lambda}_0^T L_0 \bar{N} L_0^T \boldsymbol{\lambda}_0 \tag{48}$$

Using Eq. (20) and Eq. (42) yields the following expression for the cost:

$$J^* = \frac{1}{2}(M_T\mathbf{x}_T - M_0\mathbf{x}_0)^T \bar{N}^{-1}(M_T\mathbf{x}_T - M_0\mathbf{x}_0) \tag{49}$$

Since $J^* \geq 0$ for all possible choices of initial and final conditions, it follows that $\bar{N}^{-1} \geq 0$. In fact, $J^* = 0$ implies that either 1) $M_T\mathbf{x}_T = M_0\mathbf{x}_0$, or, 2) $\bar{N}^{-1}$ has at least one eigenvalue that is zero. The first case is only possible if $\mathbf{x}_T = \Phi_{xx}(f_T, f_0)\mathbf{x}_0$, or if the desired final states arise from the natural evolution of the system from the initial states. The second condition implies that at least one eigenvalue of $\bar{N}$ is infinity. Since N comprises only bounded periodic terms and an increasing function $K(f)$, this must mean $K(f_T) \to \infty$ and consequently, $f_T \to \infty$. This is also intuitive from the physics of the problem, since in both the cases, control required is zero. Therefore, in all other cases where nonzero control is required, $\{\bar{N}, \bar{N}^{-1}\} > 0$. Furthermore, since $\bar{N}$ is symmetric and block diagonal in structure, considerable computation time can be saved by the use of methods such as the Choleskey decomposition to find its inverse.

FEEDBACK RENDEZVOUS SCHEME FOR THE NONLINEAR SYSTEM

This section of the paper deals with the main problem of interest. The rendezvous problem is solved as a neighboring optimal control problem (OCP) utilizing the closed-form reference solution developed in the previous section. Issues such as sensor and actuator modeling, noise and filtering, plume impingement, etc. are beyond the scope of this paper. In essence, the availability of the closed-form reference solution for $\varepsilon = 0$ is used to compute the feedback control solution for the case when $\varepsilon \neq 0$ by formulating a non-autonomous LQ problem with terminal constraints. The LQ problem can be solved

either by using a sweep method and storing the required gain matrices or, by repeatedly solving the resulting Hamiltonian system in real-time, for the costates at the current time. The solution for the current costate vector is utilized to compute the current control command. The second approach is more direct if the computation indeed can be achieved with speed and accuracy, as the need for storage of the time-varying gain matrices is eliminated. An example of the second method of solution using the pseudospectral method is discussed in Ref. 41. In this paper, the first approach, i.e., the sweep method is treated in a novel framework.

Continuous Control

As mentioned before, the focus of this paper is the solution of the OCP involving the TH equations, Eq. (6) with $\varepsilon \neq 0$. The Hamiltonian can be written as:

$$H = \frac{1}{2}\mathbf{u}^T R\mathbf{u} + \boldsymbol{\lambda}^T \left[\mathbf{h}(\mathbf{x}, f) + B(f)\mathbf{u}\right] \tag{50}$$

The necessary conditions for optimality are:

$$\boldsymbol{\lambda}' = -H_x \tag{51}$$

$$\mathbf{x}' = H_\lambda \tag{52}$$

and

$$H_u = 0 \tag{53}$$

Let $\mathbf{x}_{ref}$, $\mathbf{u}_{ref}$ and $\boldsymbol{\lambda}_{ref}$ indicate the reference state, control, and costate vectors, respectively.

Equations (51-53) can be approximated by the following linear differential equations where all the partial derivatives are taken along the reference trajectory:

$$\mathbf{x}' = H_{\lambda x}\mathbf{x} + H_{\lambda u}\mathbf{u} + \mathbf{m}_1 \tag{54}$$

$$\boldsymbol{\lambda}' = -[H_{xx}\mathbf{x} + H_{xu}\mathbf{u} + H_{x\lambda}\boldsymbol{\lambda} + \mathbf{m}_2] \tag{55}$$

$$\mathbf{u} = -H_{uu}^{-1}[H_{ux}\mathbf{x} + H_{u\lambda}\boldsymbol{\lambda} + \mathbf{m}] \tag{56}$$

where, $\mathbf{m}_1, \mathbf{m}_2$ and $\mathbf{m}$ are functions of true anomaly, given as,

$$\mathbf{m}_1 = H_\lambda - H_{\lambda x}\mathbf{x}_{ref} - H_{\lambda u}\mathbf{u}_{ref} \tag{57}$$

$$\mathbf{m}_2 = H_x - H_{xx}\mathbf{x}_{ref} - H_{xu}\mathbf{u}_{ref} - H_{x\lambda}\boldsymbol{\lambda}_{ref} \tag{58}$$

$$\mathbf{m} = H_u - H_{ux}\mathbf{x}_{ref} - H_{uu}\mathbf{u}_{ref} - H_{u\lambda}\boldsymbol{\lambda}_{ref} \tag{59}$$

Analytical expressions for the partial derivatives are given in Appendix II.

The Optimal Feedback Solution

The feedback solution for the linear two-point boundary value problem defined by Eqs. (54-59) can be constructed by using the backward sweep method in a way similar to that given in Ref. 39. The key steps are the substitutions

$$\boldsymbol{\lambda} = S\mathbf{x} + P\boldsymbol{\nu} + G \tag{60}$$

where ν is a terminal Lagrange multiplier associated with the terminal constraint

$$\psi = C\mathbf{x}(f) \tag{61}$$

and the following representation of ψ:

$$\psi = P^T\mathbf{x} + V\boldsymbol{\nu} + \underline{L} \tag{62}$$

where $S, P, V, \underline{L}$ and G are true anomaly dependent gain matrices. Equation (62) is utilized to eliminate $\boldsymbol{\nu}$ in terms of the states. Utilizing Eqs. (60-62) in Eqs. (54-56) and following the application of the sweep method, the optimal feedback control law can be written as

$$\mathbf{u}^* = -H_{uu}^{-1}\left[[H_{u\lambda}\{S - PV^{-1}P^T\} + H_{ux}]\mathbf{x} + H_{u\lambda}[PV^{-1}(\psi - \underline{L}) + G] + \mathbf{m}\right] \tag{63}$$

The differential equations for the gains are given below:

$$
\begin{aligned}
&S' + S\underline{A} + \underline{A}^T S + S\underline{C}S + \underline{D} = 0 \ \{\text{Riccati Equation}\} \\
&P' + [S\underline{C} + \underline{A}^T]P = 0 \\
&G' + [S\underline{C} + \underline{A}^T]G + \underline{K} = 0 \\
&V' + P^T \underline{C} P = 0 \\
&\underline{L}' + P^T [\underline{C}G + \mathbf{m}_1 - H_{\lambda u} H_{uu}^{-1} \mathbf{m}] = 0
\end{aligned}
\tag{64}
$$

where,

$$
\begin{aligned}
&\underline{A} = H_{\lambda x} - H_{\lambda u} H_{uu}^{-1} H_{ux} \\
&\underline{C} = -H_{\lambda u} H_{uu}^{-1} H_{u\lambda} \\
&\underline{D} = H_{xx} - H_{xu} H_{uu}^{-1} H_{ux} \\
&\underline{K} = S\mathbf{m}_1 + \mathbf{m}_2 - [H_{xu} + SH_{\lambda u}] H_{uu}^{-1} \mathbf{m}
\end{aligned}
\tag{65}
$$

The boundary conditions for these equations are given by the transversality conditions [39] as given below:

$$
S(f_T) = 0; P(f_T) = C^T; G(f_T) = 0; V(f_T) = 0; \underline{L}(f_T) = 0 \tag{66}
$$

The gains equations given by Eqs. (64) can be integrated backward, with f as the independent variable. In this work, the gain equations were integrated by using the MATLAB® integrator 'ode45' within an accuracy of 10^{-9}. The results were stored, and used for the propagation of the closed-loop nonlinear system. Cubic spline interpolation is utilized to provide the values of the gain matrices stored at a finite number of true anomaly values.

NUMERICAL RESULTS AND DISCUSSION

The availability of an analytical solution to the LQ problem for $\varepsilon = 0$ leads to the examination of the dependence of the cost-to-go on the final true anomaly. Since the control and costates are known analytically, the Hamiltonian of the system reduces to a

function of one implicit variable, f. Therefore, solving for the zeros of the Hamiltonian provides a necessary condition for the maneuver with the smallest true anomaly change. In this case, solving this equation is particularly difficult due to its complicated nature, because the true anomaly expresses itself through various orders of harmonics. However, additional insight into the problem may be obtained by studying Fig. 1. In this figure, a sample rendezvous from $\mathbf{x}_0 = [0;1;0;0.5;0;1]^T$ to $\mathbf{x}_T = [0;2;0;1;0;2]^T$ is chosen, with $f_0 = 35^\circ$. The figure shows the value of the cost-to-go, scaled by the maximum cost, as a function of the eccentricity of the reference, and the final value of the true anomaly. The following features of the rendezvous cost are observed:

1. The cost-to-go decreases as the final value of the true anomaly (and consequently, final time of the rendezvous) increases. This is a consequence of the fact that the matrix $\bar{N}$ comprises the growth term $K(f)$, and the cost is a function of $\bar{N}^{-1}$.
2. Depending on the final value of the true anomaly, the cost for rendezvous can be significantly high. For example, for a circular or near-circular orbit, it is best to wait for the completion of the target's orbit about the gravitational center, to obtain lower costs.
3. The behavior of the cost-to-go with changing eccentricity is an example of pitchfork bifurcation. For low eccentricities, it is observed that the rendezvous may be performed with minimal cost if the final time is such that the rendezvous is performed in intervals of complete orbits. However, for highly eccentric orbits, new minima appear approximately halfway between complete orbits. For this particular example, these correspond to regions near the apogee.

Two examples are presented to show the performance of the feedback scheme for optimal rendezvous.

Case A: Reference Orbit with Eccentricity e=0.5

In order to ensure that arbitrary choices of the semimajor axis do not lead to physically meaningless orbits, the radius at perigee, r_p, is fixed at 7,100 km. The other parameters are chosen as: $\rho_0 = 100$ Km., $f_0 = 0$, $f_T = 4\pi$, $\mathbf{x}_0 = [0;1;0;0.5;0;1]^T$ and $\mathbf{x}_T = [0;0;0;0;0;0]^T$. For the data given for this example, $\varepsilon = 0.0094$. The analytical solution to Eqs. (54-56) for $\varepsilon = 0$, is used as the reference and it is computed analytically as developed earlier in this paper. The gains are stored after performing the backward integration and the actual nonlinear system, Eq. (6) is propagated with the designed optimal feedback control law. Except for the cost-to-go, which is nondimensional, units for position and control acceleration are in kilometers and m/sec^2, respectively.

In Fig. 2a, shows the relative trajectory in the rotating frame attached to the target; the green circle marks the initial relative position of the satellite with respect to the target. The reference trajectory is shown using a dot-dash blue line. The optimal trajectory accounting for nonlinear differential gravity is indicated by the dotted, red line and is obtained by applying the optimal feedback control law. The dashed black line shows the result of applying the analytical solution for the control obtained from the linear problem with $\varepsilon = 0$. The resultant trajectories are compared with the trajectory from the open-loop solution to the nonlinear problem, which is obtained using a shooting method. This is shown in Fig 2b. The blue solid line shows the scalar distance error between the trajectory using the analytical control for the LQ problem and the open-loop

solution, and the green broken line shows the same between the trajectory from the updated feedback law, and the open-loop solution. The use of the updated feedback law results in a trajectory that is significantly different from that obtained using the analytical control law, and it more closely matches the open-loop solution. Furthermore, the terminal constraint is satisfied with an error that is many orders less than 1mm, and is therefore negligible when compared to the error from the analytical law, which is approximately 10cm. The nonlinear effects can be discerned form the differences between the optimal trajectory and the reference solution. Optimal control histories for the open-loop, feedback, and the reference solutions are shown in Fig. 2c. It is observed that the optimal feedback control matches with the open-loop optimal solution quite well whereas the reference control shows deviations, especially in the radial and along-track directions. It is also observed that most of the control is applied whenever the target crosses its apogee ($f = \pi$ and $f = 3\pi$). Fig. 2d shows a comparison between the normalized cost-to-go for the feedback and open-loop solutions. It is clear from the scale of Fig. 2d that there is essentially no difference between the two results.

Case B: Reference Orbit with Eccentricity e=0.9

As a second example, a reference orbit with e=0.9 is chosen. The remaining parameters are: $r_p = 7100$ Km , $\rho_0 = 10$ Km, $f_0 = 35\pi/180$, $f_T = 2\pi$. The initial and final conditions for this example are $\mathbf{x}_0 = [0;1;0;0.5;0;1]^T$ and $\mathbf{x}_T = [0;2;0;1;0;1]^T$. Even though this example corresponds to $\varepsilon = 0.0016$, it should be noted that the term $(1+e\cos f)$ in the denominator of Eqs. (10)-(12) will magnify the effects of nonlinearity for such a highly eccentric orbit. The relative trajectory using the control laws developed is shown in Fig. 3a. Figure 3b shows the trajectory distance errors between the analytical control

law and the optimal feedback law, with respect to the open-loop solution, respectively. The blue solid line, that indicates the error between the trajectory using the analytical law and the open-loop solution, results in a terminal position error of more than 10m. The resulting error using the optimal feedback law, as shown by the green broken line, is approximately 50mm, at the terminal point. This figure, therefore, clearly shows the advantage of using the optimal control law. In this case, as is shown in Fig.3c, the optimal feedback results are compared with the open-loop solution. It has been found that solving the open-loop problem by using shooting methods is very sensitive to the initial guess. The feedback scheme not only helps in the correction of the reference solution, but also finds the correct initial guess for intractable problems such as this case.

CONCLUSIONS

An optimal feedback control methodology is presented for minimum-fuel rendezvous near elliptic orbits accounting for nonlinear differential gravity. The rendezvous problem for the nonlinear differential gravity model is solved by the application of neighboring optimal feedback control methodology used in conjunction with a nominal trajectory, obtained by solving the related minimum-fuel feedback control problem for the linear Tschauner-Hempel equations, analytically. The analytical solution also provides remarkable insight into the cost of rendezvous and its dependence on true anomaly, especially for eccentric orbits. The process is facilitated through the use of a novel perturbation parameter, which simultaneously captures the effects of eccentricity and nonlinearity. Several numerical examples are analyzed to demonstrate the efficacy of the method and the results are compared with those obtained from open-loop calculations.

References

[1] Hill, G.W., "Researches in the Lunar Theory", *American Journal of Mathematics*, Vol.1, No.1, 1878, pp. 5-26.

[2] Clohessy, W. H. and Wiltshire, R. S., "Terminal Guidance System for Satellite Rendezvous," *Journal of the Aerospace Sciences*, Vol. 27, September 1960, pp. 653–658, 674.

[3] Knollman, G. C. and Pyron, B. O., "Relative Trajectories of Objects Ejected from a Near Satellite," *AIAA Journal*, Vol. 1, No. 2, February 1963, pp. 424–429.

[4] London, H. S., "Second Approximation to the Solution of Rendezvous Equations," *AIAA Journal*, Vol. 1, No. 7, July 1963, pp. 1691–1693.

[5] Karlgaard, C. D. and Lutze, F. H., "Second-Order Relative Motion Equations," *Journal of Guidance, Control, and Dynamics*, Vol. 26, No. 1, January-February 2003, pp. 41–49.

[6] Richardson, D. L. and Mitchell, J. W., "A Third-Order Analytical Solution for Relative Motion with a Circular Reference Orbit," *The Journal of the Astronautical Sciences*, Vol. 51, No. 1, January-March 2003, pp. 1–12.

[7] Tschauner, J. and Hempel, P., "Rendezvous zu einemin Elliptischer Bahn umlaufenden Ziel," *Astronautica Acta*, Vol. 11, No. 2, 1965, pp. 104–109.

[8] de Vries, J. P., "Elliptic Elements in Terms of Small Increments of Position and Velocity Components," *AIAA Journal*, Vol. 1, No. 11, November 1963, pp. 2626– 2629.

[9] Lawden, D. F., *Optimal Trajectories for Space Navigation*, Butterworths, London, UK, 1967, pp. 79–95.

[10] Carter, T. E. and Humi, M., "Fuel-Optimal Rendezvous Near a Point in General Keplerian Orbit," *Journal of Guidance, Control, and Dynamics*, Vol. 10, No. 6, November-December 1987, pp. 567–573.

[11] Carter, T. E., "New Form for the Optimal Rendezvous Equations Near a Keplerian Orbit," *Journal of Guidance, Control, and Dynamics*, Vol. 13, No. 1, January- February 1990, pp. 183–186.

[12] Wolfsberger, W., Weiß, J., and Rangnitt, D., "Strategies and Schemes for Rendezvous on Geostationary Transfer Orbit," *Acta Astronautica*, Vol. 10, No. 8, August 1983, pp. 527–538.

[13] Carter, T. E., "State Transition Matrices for Terminal Rendezvous Studies: Brief Survey and New Examples," *Journal of Guidance, Control, and Dynamics*, Vol. 21, No. 1, January-February 1998, pp. 148–155.

[14] Yamanaka, K. and Ankersen, F., "New State Transition Matrix for Relative Motion on an Arbitrary Elliptical Orbit," *Journal of Guidance, Control, and Dynamics*,Vol. 25, No. 1, January-February 2002, pp. 60–66.

[15] Garrison, J. L., Gardner, T. G., and Axelrad, P., "Relative Motion in Highly Elliptical Orbits," *Advances in the Astronautical Sciences*, Vol. 89(2), Univelt Inc., 1995, pp. 1359–1376, Paper AAS 95-194.

[16] Melton, R. G., "Time Explicit Representation of Relative Motion Between Elliptical Orbits," *Journal of Guidance, Control and Dynamics*, Vol. 23, No. 4, July-August 2000, pp. 604–610.

[17] Broucke, R. A., "Solution of the Elliptic Rendezvous Problem with the Time as Independent Variable," *Journal of Guidance, Control, and Dynamics*, Vol. 26, No. 4, July-August 2003, pp. 615–621.

[18] Euler, E. A. and Shulman, Y., "Second-Order Solution to the Elliptic Rendezvous Problem," *AIAA Journal*, Vol. 5, No. 5, May 1967, pp. 1033–1035.

[19] Sengupta, P., Sharma, R., and Vadali, S. R., "Periodic Relative Motion Near a General Keplerian Orbit with Nonlinear Differential Gravity," *Journal of Guidance, Control, and Dynamics*, (to appear).

[20] Billik, B. H., "Some Optimal Low-Acceleration Rendezvous Maneuvers," *AIAA Journal*, Vol. 2, No. 3, March 1964, pp. 510–516.

[21] Euler, E. A., "Optimal Low-Thrust Rendezvous Control," *AIAA Journal*, Vol. 7, No. 6, June 1969, pp. 1140–1144.

[22] Edelbaum, T. N., "Optimum Low-Thrust Rendezvous and Stationkeeping," *AIAA Journal*, Vol. 2, No. 7, July 1964, pp. 1196–1201.

[23] Gobetz, F. W., "Linear Theory of Optimum Low-Thrust Rendezvous Trajectories," *The Journal of the Astronautical Sciences*, Vol. 12, No. 3, Fall 1965, pp. 69–76.

[24] Broucke, R. A. and Cefola, P. J., "On the Equinoctial Orbit Elements," *Celestial Mechanics*, Vol. 5, 1972, pp. 303–310.

[25] Jezewski, D. J. and Stoolz, J. M., "A Closed-form Solution for Minimum-Fuel, Constant-Thrust Trajectories," *AIAA Journal*, Vol. 8, No. 7, July 1970, pp. 1229–1234.

[26] Carter, T. E. and Brient, J., "Fuel-Optimal Rendezvous for Linearized Equations of Motion," *Journal of Guidance, Control, and Dynamics*, Vol. 15, No. 6, November-December 1992, pp. 1411–1416.

[27] Humi, M., "Fuel-Optimal Rendezvous in a General Central Gravity Field," *Journal of Guidance, Control, and Dynamics*, Vol. 16, No. 1, January-February 1993, pp. 215–217.

[28] Zanon, D. J. and Campbell, M. E. "Optimal planner for Spacecraft Formations in Elliptical Orbits", *Journal of Guidance, Control, and Dynamics*, Vol. 29, No. 1, Jan–Feb. 2006, pp. 161-171.

[29] Palmer, P., "Optimal Relocation of Satellites Flying in Near-Circular-Orbit Formations" *Journal of Guidance, Control, and Dynamics*, Vol. 29, No. 3, May–June 2006, pp. 519-526.

[30] Williams, P., "Spacecraft Rendezvous on Small Relative Inclination Orbits using Tethers", *AIAA/AAS Astrodynamics Specialist Conference and Exhibit*, No. AIAA-2004-5310*,* Providence, Rhode Island, Aug. 16-19, 2004.

[31] Park, C. Guibout, V. and Scheeres, D. J., "Solving Optimal Continuous Thrust Rendezvous Problems with Generating Functions" *Journal of Guidance, Control, and Dynamics*, Vol. 29, No. 2, March–April 2006, pp. 321-331.

[32] Kim, Y. H. and Spencer, D. B., " Optimal Spacecraft Rendezvous Using Genetic Algorithms" *Journal of Guidance, Control, and Dynamics*, Vol. 39, No. 6, Nov–Dec. 2002, pp. 859-865.

[33] Curtis, S. A., "The Magnetosphere Multiscale Mission... Resolving Fundamental Processes in Space Plasmas," Tech. Rep. NASA TM-2000-209883, NASA Science and Technology Definition Team for the MMS Mission, 1999.

[34] Carpenter, J. R., Leitner, J. A., Folta, D. C., and Burns, R. D., "Benchmark Problems for Spacecraft Formation Flight Missions," *AIAA Guidance, Navigation, and Control Conference and Exhibit*, No. AIAA-2003-5364, AIAA, Austin, TX, August 2003.

[35] Pesch, H. J., "Numerical Computation of Neighboring Optimum Feedback Control Schemes in Real-time", *Applied Mathematics and Optimization*, Vol. 5, No. 1, March 1979, pp. 231-252.

[36] Foerster, R. E. and Flugge-Lotz, I., "A Neighboring Optimal Feedback Control Scheme for Systems Using Discontinuous Control" , *Journal of Optimization Theory and Applications*, Vol. 8, No. 5, Nov. 1971, pp. 367-395.

[37] Wetzel, T. A., Moeder, D. D. and Pierson, B. L. "Performance of a Second-order Neighboring Optimal Control Scheme" , *AIAA Guidance, Navigation and Control Conference,* , No. AIAA-96-3707*,* San Diego, CA, July. 29-31, 1996.

[38] Marec, J-P., *Optimal Spacecraft Trajectories, Studies in Astronautics*, Vol. 1, Elsevier Scientific Publishing Company, The Netherlands, 1979, pp. 7-19.

[39] Bryson, A. E. and Ho, Y.-C., *Applied Optimal Control*, Hemisphere Publishing Co., Washington, D.C., 1975, pp. 158-164.

[40] Battin, R. H., *An Introduction to the Mathematics and Methods of Astrodynamics*, *AIAA Education Series,* American Institute of Aeronautics and Astronautics, Inc., Reston, VA, Revised Ed., 1999, pp. 158-159.

[41] Yan, H. and Alfriend, K. T., "Three-axis Magnetic Attitude Control using Pseudospectral Control Law in Eccentric Orbits." AAS 06-103, *AAS/AIAA Space Flight Mechanics Conference*, Tampa, FL, Jan 2006.

List of Figures

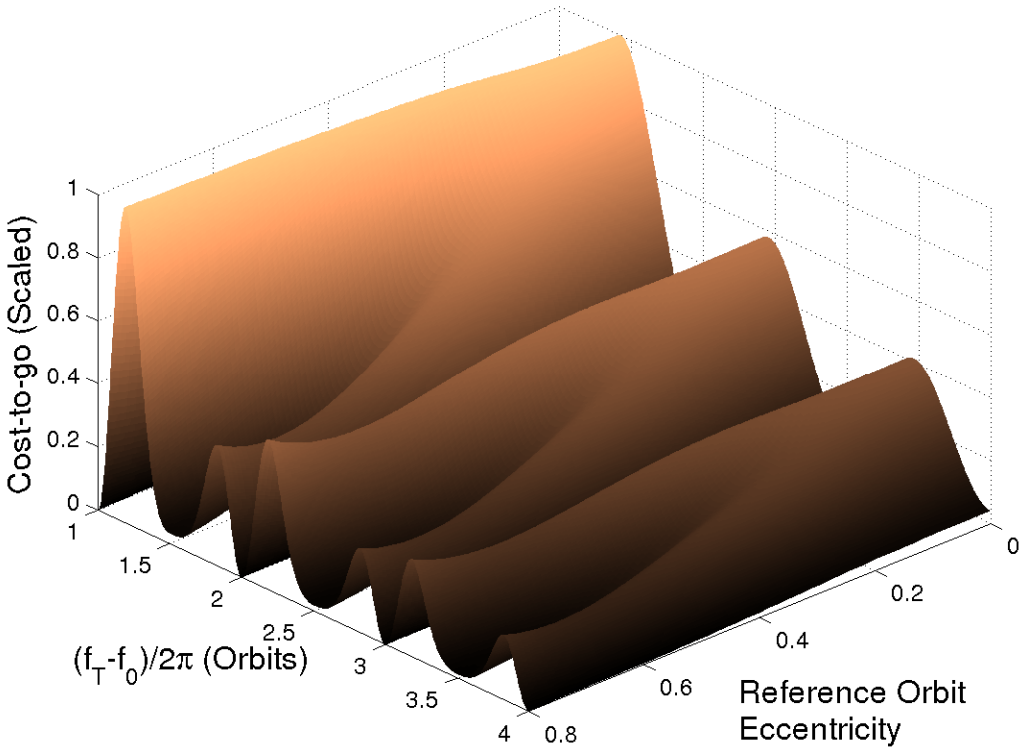

Fig.1: The Cost-to-go as a Function of the Eccentricity of the Reference, and the Final Value of the True Anomaly.

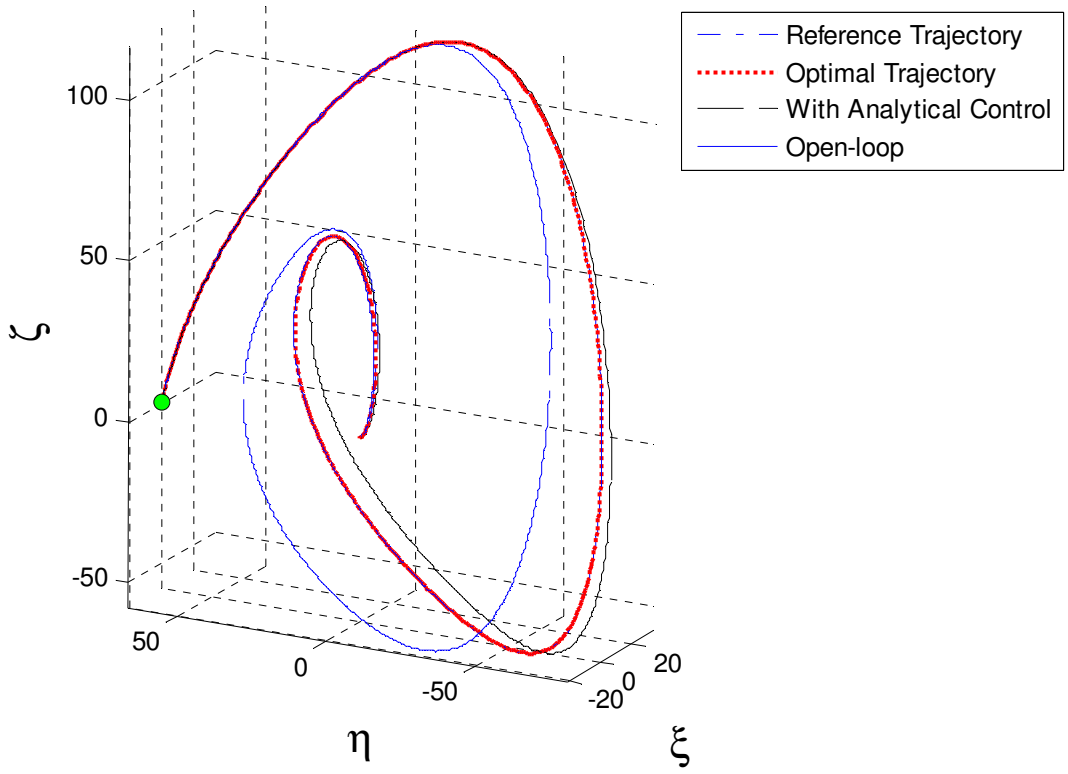

Fig.2a: Case A (e=0.5) Reference Solution and the Optimal Relative Trajectory (in km).

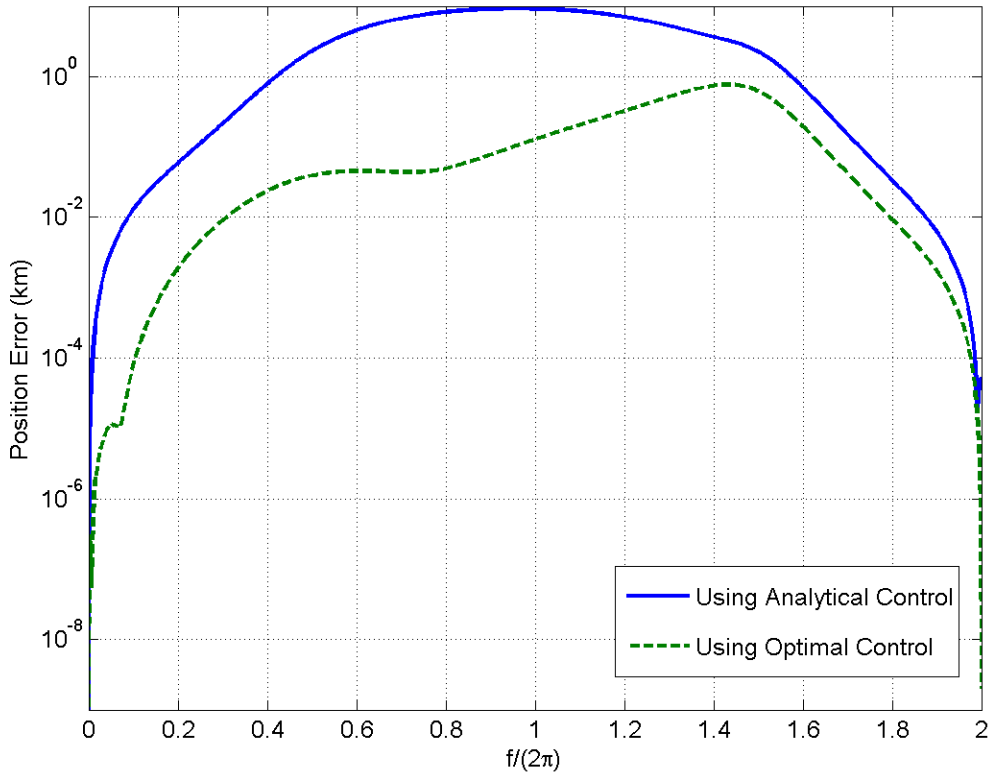

Fig. 2b: Case A (e=0.5) Position Errors in Trajectory from Analytical and the Optimal Feedback Law.

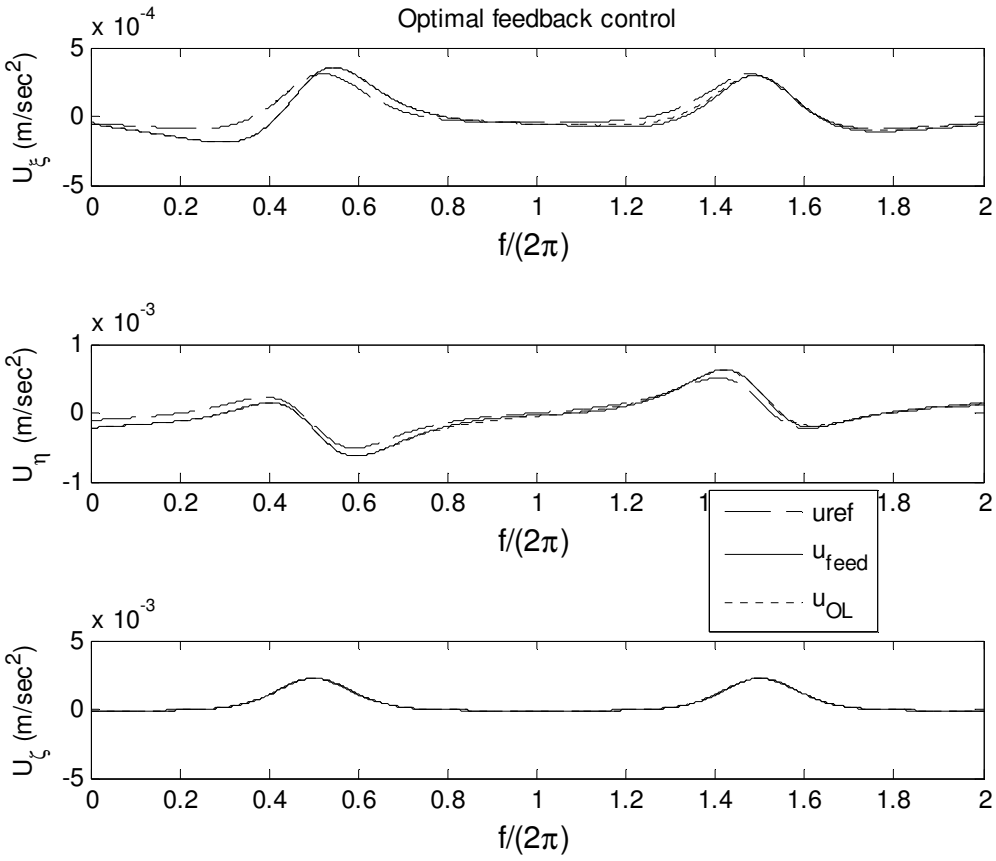

Fig.2c: Case A (e=0.5) Reference, the Feedback and Open-loop Optimal Control Histories.

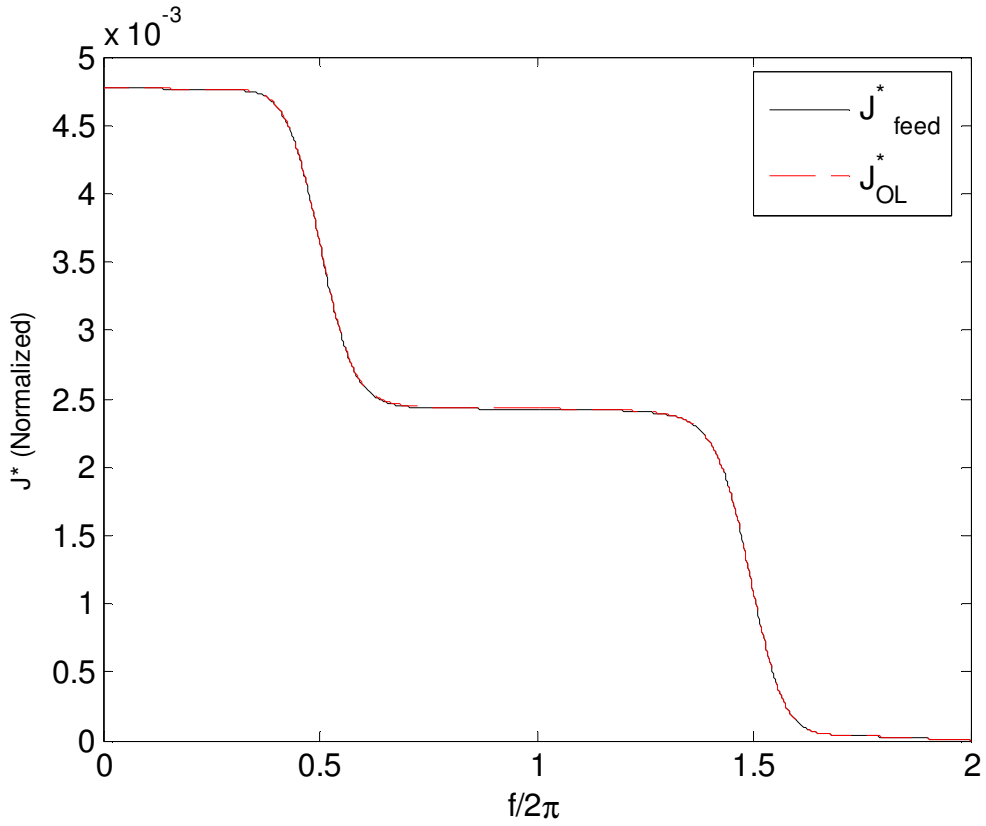

Fig. 2d: Case A (e=0.5) Comparison of Nondimensional, Open-Loop and Feedback Cost-to-go.

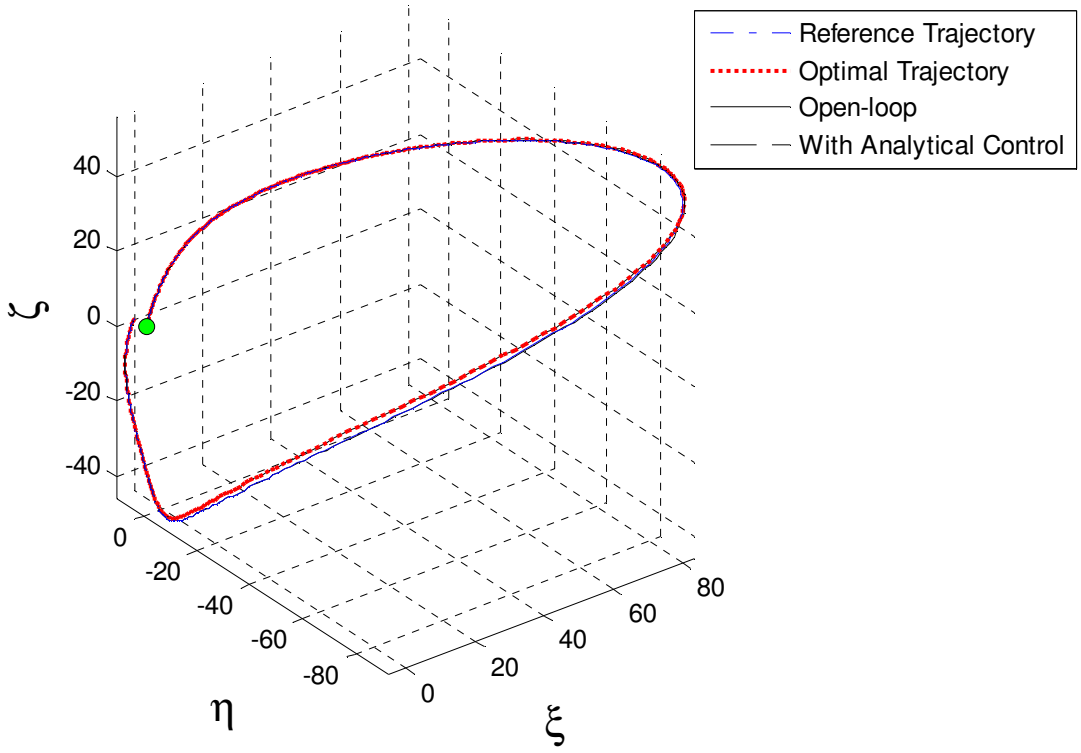

Fig.3a: Case B (e=0.9) Reference Solution and the Optimal Relative Trajectory (in km).

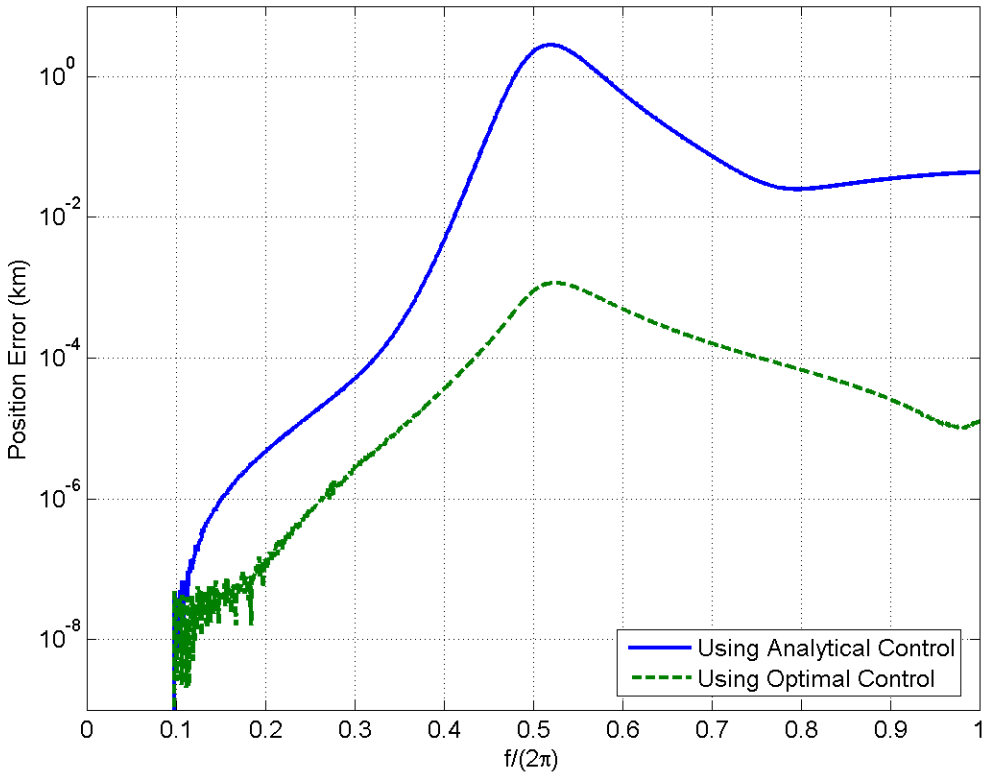

Fig. 3b: Case B (e=0.9) Position Errors in Trajectory from Analytical and the Optimal Feedback Law.

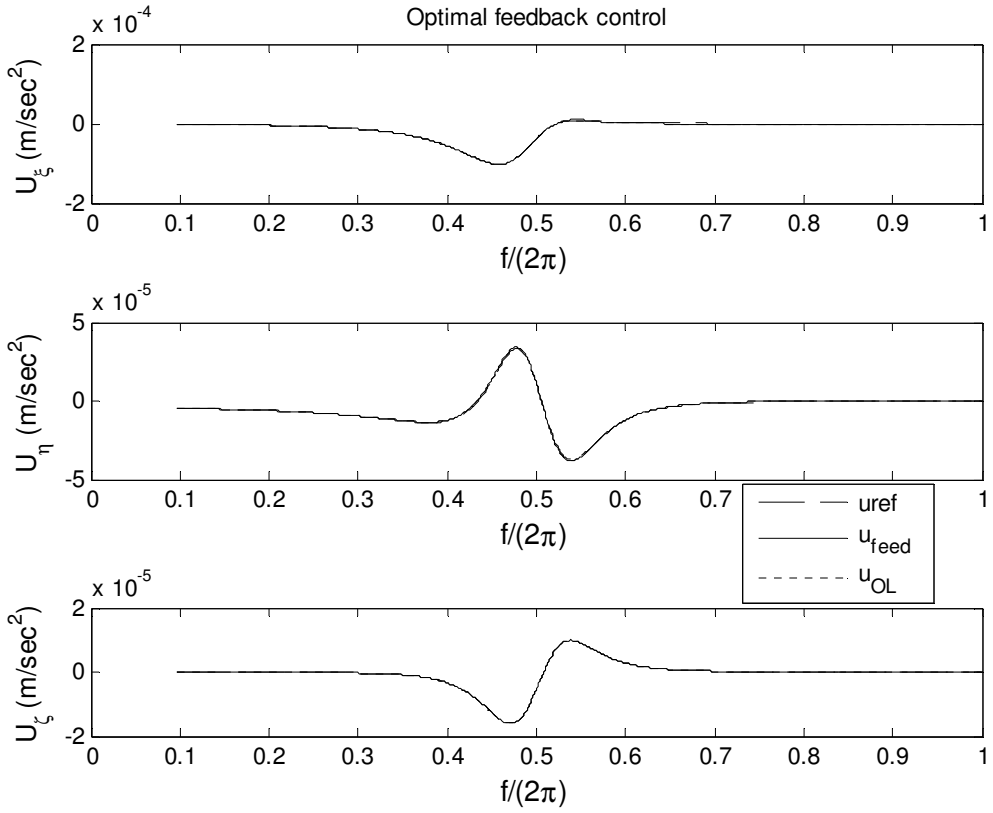

Fig. 3c: Case B (e=0.9) Reference, the Feedback and Open-loop Optimal Control Histories.

APPENDIX I

By denoting $r_i = \frac{1}{R_i}$, the non-zero components of $N^{(0..3)}(f)$ are:

$$N_{44}^{(3)} = \frac{3}{2}\frac{e^2 r_1}{\eta^{15}} + 3\frac{r_2}{\eta^{13}}, \quad N_{24}^{(3)} = eN_{44}^{(3)}, \quad N_{22}^{(3)} = e^2 N_{44}^{(3)}$$

$$N_{44}^{(2)} = -\frac{3}{4}\frac{e^2 r_1}{\eta^{12}}\frac{\sin f\,(5e + 6\cos f + e\cos 2f)}{(1+e\cos f)^3}$$

$$N_{34}^{(2)} = \frac{3}{2\eta^8}\left(\frac{e^2}{2\eta^2} r_1 + r_2\right)$$

$$N_{14}^{(2)} = -\frac{3}{4\eta^{12}}\frac{e}{}\left(r_1 - 5r_2\right)$$

$$N_{24}^{(2)} = eN_{44}^{(2)}, \quad N_{12}^{(2)} = eN_{14}^{(2)}, \quad N_{22}^{(2)} = eN_{24}^{(2)}, \quad N_{32}^{(2)} = eN_{34}^{(2)}$$

$$N_{66}^{(1)} = \frac{1}{8}\frac{\left(4 + 41e^2 + 18e^4\right) r_3}{\eta^{11}}, \quad N_{55}^{(1)} = \frac{1}{8}\frac{\left(4 + 3e^2\right) r_3}{\eta^9}$$

$$\begin{aligned} N_{44}^{(1)} = {} & \frac{r_1}{16\eta^{15}(1+e\cos f)^4}[e^3\left(32e^8 - 260e^6 + 273e^4 + 876e^2 + 80\right)\left(\frac{e}{8}\cos 4f + \cos 3f\right) \\ & + \frac{e^2}{2}\left(32e^{10} - 20e^8 - 1503e^6 + 2874e^4 + 5072e^2 + 552\right)\cos 2f \\ & + e\left(96e^{10} - 588e^8 - 541e^6 + 4296e^4 + 3296e^2 + 448\right)\cos f \\ & + \left(12e^{12} + \frac{45}{2}e^{10} - \frac{6477}{8}e^8 + \frac{2503}{2}e^6 + 2583e^4 + 1256e^2 + 64\right)] \\ & + \frac{r_2}{8\eta^{13}(1+e\cos f)^3}[\frac{e^2}{2}\left(2e^6 - 41e^4 + 76e^2 + 40\right)\left(\frac{e}{2}\cos 3f + 3\cos 2f\right) \\ & + \frac{3e}{4}\left(2e^8 - e^6 - 184e^4 + 440e^2 + 128\right)\cos f + \frac{e^2}{2}\left(6e^6 - 39e^4 - 94e^2 + 512\right)] \end{aligned}$$

$$N_{34}^{(1)} = \frac{\eta^5}{3}N_{44}^{(2)}, \quad N_{33}^{(1)} = \frac{2\eta^5}{3}N_{34}^{(2)}$$

$$N_{24}^{(1)}=-\frac{er_1}{16\eta^{15}(1+e\cos f)^4}[e\left(70e^8-113e^6-746e^4-220e^2+8\right)\left(\frac{e}{8}\cos 4f+\cos 3f\right)$$
$$+\frac{1}{2}\left(46e^{10}+403e^8-1544e^6-4672e^4-1264e^2+24\right)\cos 2f$$
$$+e\left(178e^8+101e^6-2946e^4-3516e^2-824\right)\cos f$$
$$+\frac{1}{8}\left(114e^{10}+2237e^8-6662e^6-17004e^4-12504e^2-1216\right)]$$
$$+\frac{r_2}{8\eta^{13}(1+e\cos f)^3}[-\frac{e}{2}\left(13e^6-4e^4-66e^2-20\right)\left(\frac{e}{2}\cos 3f+3\cos 2f\right)$$
$$+\left(\frac{9}{4}e^8-60e^6+\frac{123}{2}e^4+237e^2+48\right)\cos f+\frac{e}{2}\left(e^6-94e^4+206e^2+272\right)]$$

$$N_{23}^{(1)}=\frac{e\eta^5}{3}N_{44}^{(2)}$$

$$N_{22}^{(1)}=-\frac{r_1}{16\eta^{15}(1+e\cos f)^4}[e^3\left(113e^6+536e^4+360e^2-8\right)\left(\frac{e}{8}\cos 4f+\cos 3f\right)$$
$$+\frac{e^4}{2}\left(137e^6+1094e^4+3792e^2+1984\right)\cos 2f$$
$$+e\left(339e^8+1996e^6+3416e^4+1224e^2+32\right)\cos f$$
$$+\left(-\frac{141}{8}e^{10}+744e^8+1588e^6+1793e^4+264e^2+8\right)]$$
$$+\frac{r_2}{8\eta^{13}(1+e\cos f)^3}[-\frac{7e^2}{2}\left(4e^4-7e^2-8\right)\left(\frac{e}{2}\cos 3f+3\cos 2f\right)$$
$$+\frac{3e}{4}\left(4e^6-159e^4+348e^2+192\right)\cos f+\left(-2e^6-\frac{149}{2}e^4+253e^2+16\right)]$$

$$N_{14}^{(1)}=\frac{\sin f}{2\eta^9(1+e\cos f)^3}\left[3e\left(r_1-5r_2\right)\cos f+\frac{e^2}{2}\left(r_1-5r_2\right)\cos 2f+\frac{e^2}{2}\left(5r_1-r_2\right)-12r_2\right]$$

$$N_{11}^{(1)}=\frac{1}{2}\frac{r_1}{\eta^9}+\frac{1}{8}\frac{\left(47e^2+16\right)r_2}{\eta^{11}},\quad N_{13}^{(1)}=\frac{2\eta^5}{3}N_{14}^{(2)},\quad N_{12}^{(1)}=eN_{14}^{(1)}$$

$$N_{66}^{(0)}=-\frac{r_3\sin f}{120\eta^8(1+e\cos f)^5}[\frac{e^2}{4}\left(190e^4+131e^2-6\right)\left(\frac{e}{2}\cos 4f+5\cos 3f\right)$$
$$+\frac{e}{2}\left(150e^6+1789e^4+1271e^2-60\right)\cos 2f$$
$$+\left(\frac{1385}{2}e^6+\frac{6365}{4}e^4+\frac{2325}{2}e^2-60\right)\cos f$$
$$+\frac{e}{8}\left(410e^6+6993e^4+7282e^2+2640\right)]$$

$$N_{55}^{(0)}=-\frac{r_3\sin f}{120\eta^6(1+e\cos f)^5}[\frac{e^2}{4}\left(29e^2+6\right)\left(\frac{e}{2}\cos 4f+5\cos 3f\right)$$
$$+\frac{e}{2}\left(21e^4+269e^2+60\right)\cos 2f+\left(\frac{395}{4}e^4+\frac{435}{2}e^2+60\right)\cos f$$
$$+\frac{e}{8}\left(247e^4+478e^2+1200\right)]$$

$$N_{56}^{(0)}=-\frac{(5e^2-1)}{80\eta^{10}}\frac{(\cos f+e)r_3}{(1+e\cos f)^5}[\frac{e^3}{2}\cos 4f-e^2\left(e^2-5\right)\cos 3f$$
$$+2e\left(e^4-4e^2+10\right)\cos 2f+\left(-4e^6+17e^4-25e^2+40\right)\cos f$$
$$+\frac{e\left(12e^6-49e^4+137e^2+40\right)}{2(5e^2-1)}$$

$$N_{44}^{(0)}=-\frac{r_1e\sin f}{240\eta^{12}\left(1+e\cos f\right)^5}[\frac{e^3}{4}\left(240e^6-2460e^4+5047e^2+2178\right)\left(\frac{e}{2}\cos 4f+5\cos 3f\right)$$
$$+\frac{e^2}{2}\left(21300+46687e^2-18357e^4+180e^6+240e^8\right)\cos 2f$$
$$+\frac{5e}{4}\left(-5556e^6+720e^8+31098e^2+893e^4+15888\right)\cos f$$
$$+\left(7680+\frac{80197}{4}e^4-\frac{76939}{8}e^6+\frac{795}{2}e^8+90e^{10}-15810e^2\right)]$$
$$+\frac{r_2e\sin f}{120\eta^{10}\left(1+e\cos f\right)^5}[\frac{e^3}{4}\left(10e^4+211e^2-606\right)\left(\frac{e}{2}\cos 4f+5\cos 3f\right)$$
$$+\frac{e^2}{2}\left(30e^6-289e^4-1591e^2+5700\right)\cos 2f+\frac{5e}{4}\left(82e^6-761e^4+198e^2+3792\right)\cos f$$
$$-\left(\frac{65}{4}e^8+\frac{47}{8}e^6+2250e^2-\frac{4261}{4}e^4+1440\right)]$$

$$N_{33}^{(0)}=\frac{\eta^{10}}{9}N_{44}^{(2)}$$

$$\begin{aligned}N_{34}^{(0)}=&-\frac{r_1 e}{12\eta^{10}(1+e\cos f)^4}[e^2\left(9e^4-20e^2-2\right)\left(\frac{e}{8}\cos 4f+\cos 3f\right)\\&-\frac{e}{2}\left(6e^8-36e^6+11e^4+89e^2+21\right)\cos 2f+\left(-8e^8+67e^6-96e^4-30e^2-24\right)\cos f\\&-\frac{e}{8}\left(24e^8-191e^6+208e^4+66e^2+348\right)]\\&-\frac{r_2 e}{6\eta^8(1+e\cos f)^3}[\frac{e}{2}\left(12e^2-5\right)\left(\frac{e}{2}\cos 3f+3\cos 2f\right)\\&+\left(18e^4+\frac{93}{4}e^2-3e^6-12\right)\cos f-\frac{e}{2}\left(10e^4-66e^2+21\right)]\end{aligned}$$

$$\begin{aligned}N_{22}^{(0)}=&-\frac{r_1\sin f}{240\eta^{12}\left(1+e\cos f\right)^5}[\frac{e^2}{4}\left(1247e^6+3318e^4+480e^2-40\right)\left(\frac{e}{2}\cos 4f+5\cos 3f\right)\\&+\frac{e}{2}\left(1143e^8+12947e^6+31920e^4+4320e^2-280\right)\cos 2f\\&+\left(\frac{19865}{4}e^8+\frac{34695}{2}e^6+27960e^4+3650e^2-120\right)\cos f\\&+\frac{e}{8}\left(61e^8+61414e^6+119520e^4+84520e^2+9760\right)]\\&+\frac{r_2\sin f}{120\eta^{10}\left(1+e\cos f\right)^5}[\frac{e^2}{4}\left(220e^4-559e^2-46\right)\left(\frac{e}{2}\cos 4f+5\cos 3f\right)\\&+\frac{e}{2}\left(60e^6+1909e^4-5419e^2-400\right)\cos 2f+\left(385e^6+\frac{2855}{4}e^4-\frac{9995}{2}e^2-240\right)\cos f\\&\frac{e}{8}\left(20e^6+5763e^4-11278e^2-15680\right)]\end{aligned}$$

$$N_{23}^{(0)}=-\frac{r_1 e}{12\eta^{10}(1+e\cos f)^4}[e\left(3e^6-6e^4-12e^2+2\right)\left(\frac{e}{8}\cos 4f+\cos 3f\right)$$
$$+\left(\frac{27}{2}e^6-\frac{75}{2}e^4-\frac{49}{2}e^2+3\right)\cos 2f+e\left(9e^6+2e^4-84e^2-18\right)\cos f$$
$$\left(\frac{69}{8}e^8-\frac{75}{4}e^6+14e^4-\frac{255}{4}e^2+3\right)]$$
$$-\frac{r_2}{6\eta^8(1+e\cos f)^3}[\frac{e}{2}\left(9e^4+3e^2-5\right)\left(\frac{e}{2}\cos 3f+3\cos 2f\right)$$
$$+\left(\frac{15}{4}e^6+\frac{153}{4}e^4-\frac{15}{4}e^2-12\right)\cos f+\frac{e}{2}\left(17e^4+57e^2-39\right)]$$

$$N_{24}^{(0)}=\frac{r_1\sin f}{240\eta^{12}\left(1+e\cos f\right)^5}[\frac{e^3}{4}\left(730e^6-2347e^4-3348e^2-40\right)\left(\frac{e}{2}\cos 4f+5\cos 3f\right)$$
$$+\frac{e^2}{2}\left(450e^8+5107e^6-23617e^4-31410e^2-580\right)\cos 2f$$
$$+\frac{5e}{4}\left(1886e^8-2513e^6-20448e^4-21248e^2-720\right)\cos f$$
$$+\left(\frac{535}{4}e^{10}+\frac{25239}{8}e^8-11488e^6-16600e^4-9130e^2-480\right)]$$
$$+\frac{r_2\sin f}{120\eta^{10}\left(1+e\cos f\right)^5}[\frac{e^3}{4}\left(115e^4-174e^2-326\right)\left(\frac{e}{2}\cos 4f+5\cos 3f\right)$$
$$+\frac{e^2}{2}\left(15e^6+1099e^4-1914e^2-3050\right)\cos 2f+\frac{5e}{4}\left(113e^6+666e^4-2098e^2-1992\right)\cos f$$
$$\left(-\frac{55}{8}e^8+\frac{1429}{4}e^6-\frac{689}{4}e^4-2105e^2-720\right)]$$

$$N_{11}^{(0)}=-\frac{r_1\sin f}{12\eta^6(1+e\cos f)^3}\left(5e+6\cos f+e\cos 2f\right)$$
$$-\frac{r_2\sin f}{120\eta^8\left(1+e\cos f\right)^5}[\frac{e^2}{4}\left(361e^2-46\right)\left(\frac{e}{2}\cos 4f+5\cos 3f\right)$$
$$+\frac{e}{2}\left(249e^4+3301e^2-400\right)\cos 2f+\left(\frac{4735}{4}e^4+\frac{4885}{2}e^2-240\right)\cos f$$
$$+\frac{e}{8}\left(443e^4+13362e^2+3520\right)]$$

$$N_{12}^{(0)}=\frac{r_1}{12\eta^{12}(1+e\cos f)^4}[e\left(3e^6-6e^4-12e^2+2\right)\left(\frac{e}{8}\cos 4f+\cos 3f\right)$$
$$+\frac{1}{2}\left(27e^6-75e^4-49e^2+6\right)\cos 2f+e\left(9e^6+2e^4-84e^2-18\right)\cos f$$
$$+\left(\frac{69}{8}e^8-\frac{75}{4}e^6+14e^4-\frac{255}{4}e^2+3\right)]$$
$$-\frac{r_2}{60\eta^{12}(1+e\cos f)^5}[\frac{e^2}{8}\left(75e^6+450e^4+75e^2+23\right)\left(\frac{e}{2}\cos 5f+5\cos 4f\right)$$
$$+\frac{5e}{16}\left(111e^8+966e^6+3711e^4+659e^2+160\right)\cos 3f$$
$$+\left(270e^8+\frac{2615}{2}e^6+2520e^4+515e^2+60\right)\cos 2f$$
$$+\frac{5e}{8}\left(81e^8+1752e^6+5017e^4+5225e^2+1008\right)\cos f$$
$$+\frac{1}{8}\left(1449e^8+10370e^6+16105e^4+10845e^2+480\right)]$$

$$N_{13}^{(0)}=\frac{\eta^5}{3}N_{14}^{(1)}$$

$$N_{14}^{(0)}=\frac{r_1}{12\eta^{12}(1+e\cos f)^4}[e^2\left(9e^4-20e^2-2\right)\left(\frac{e}{8}\cos 4f+\cos 3f\right)$$
$$\frac{e}{2}\left(6e^8-36e^6+11e^4+89e^2+21\right)\cos 2f+\left(-8e^8+67e^6-96e^4-30e^2-24\right)\cos f$$
$$-\frac{e}{8}\left(24e^8-191e^6+208e^4+66e^2+348\right)]$$
$$+\frac{r_2}{60\eta^{12}(1+e\cos f)^5}[-\frac{e^3}{8}\left(105e^4+355e^2+163\right)\left(\frac{e}{2}\cos 5f+5\cos 4f\right)$$
$$+\frac{5e^2}{16}\left(24e^8-261e^6-871e^4-3279e^2-1220\right)\cos 3f$$
$$+\frac{5e}{2}\left(22e^8-248e^6-268e^4-1126e^2-249\right)\cos 2f$$
$$+\frac{1}{8}\left(300e^{10}-1135e^8-11685e^6-14825e^4-35190e^2-2880\right)\cos f$$
$$+\frac{e}{8}\left(656e^8-4995e^6-4505e^4-18585e^2-11820\right)]$$

APPENDIX II

From the Hamiltonian defined by Eq. (50), it follows that:

$$H_u = R\mathbf{u} + B^T\boldsymbol{\lambda}$$
$$\Rightarrow H_{uu} = R, \quad H_{u\lambda} = B^T$$

It can be shown that:

$$H_\lambda = \mathbf{h}(\mathbf{x}, f) + B\mathbf{u}$$

Finally, $$H_x = \left(\frac{\partial \mathbf{h}}{\partial \mathbf{x}}\right)^T \boldsymbol{\lambda}$$

$$\Rightarrow H_{xu} = O, \quad H_{x\lambda} = \left(\frac{\partial \mathbf{h}}{\partial \mathbf{x}}\right)^T, \quad H_{xx} = \frac{\partial}{\partial \mathbf{x}}\left(\frac{\partial \mathbf{h}}{\partial \mathbf{x}}\right)^T \boldsymbol{\lambda}$$

Clearly, only $H_{x\lambda}$ and H_{xx} need to be provided explicitly. The non-zero entries of the partial derivative matrix of $\mathbf{h}(\mathbf{x}, f)$ along the reference trajectory are given below, with the notation, $d = \left[(1+\varepsilon x)^2 + \varepsilon^2 y^2 + \varepsilon^2 z^2\right]^{1/2}$:

$$\frac{\partial h_1}{\partial v_1} = 1$$

$$\frac{\partial h_2}{\partial v_2} = 1$$

$$\frac{\partial h_3}{\partial v_3} = 1$$

$$\frac{\partial h_4}{\partial x} = \frac{1}{(1+e\cos f)}\left(1 - \frac{1}{d^3} + 3\frac{(1+\varepsilon x)^2}{d^5}\right)$$

$$\frac{\partial h_4}{\partial y} = \frac{3}{(1+e\cos f)}\frac{(1+\varepsilon x)(\varepsilon y)}{d^5}$$

$$\frac{\partial h_4}{\partial z} = \frac{3}{(1+e\cos f)}\frac{(1+\varepsilon x)(\varepsilon z)}{d^5}$$

$$\frac{\partial h_4}{\partial v_2} = 2$$

$$\frac{\partial h_5}{\partial x} = \frac{3}{(1+e\cos f)}\frac{(1+\varepsilon x)(\varepsilon y)}{d^5}$$

$$\frac{\partial h_5}{\partial y} = \frac{1}{(1+e\cos f)}\left(1-\frac{1}{d^3}+3\frac{(1+\varepsilon x)^2}{d^5}\right)$$

$$\frac{\partial h_5}{\partial z} = \frac{3}{(1+e\cos f)}\frac{(\varepsilon x)(\varepsilon z)}{d^5}$$

$$\frac{\partial h_5}{\partial v_1} = -2$$

$$\frac{\partial h_6}{\partial x} = \frac{3}{(1+e\cos f)}\frac{(1+\varepsilon x)(\varepsilon z)}{d^5}$$

$$\frac{\partial h_6}{\partial y} = \frac{3}{(1+e\cos f)}\frac{\varepsilon^2 yz}{d^5}$$

$$\frac{\partial h_6}{\partial z} = \frac{1}{(1+e\cos f)}\left(-e\cos f-\frac{1}{d^3}+3\frac{\varepsilon^2 z^2}{d^5}\right)$$